



## A fast multipole boundary element method for 2D viscoelastic problems

X.Y. Zhu<sup>a,d</sup>, W.Q. Chen<sup>b</sup>, Z.Y. Huang<sup>a,\*</sup>, Y.J. Liu<sup>c</sup>

<sup>a</sup> Department of Civil Engineering, Zhejiang University, Zijingang Campus, Hangzhou 310058, PR China

<sup>b</sup> Department of Engineering Mechanics, Zhejiang University, Yuquan Campus, Hangzhou 310027, PR China

<sup>c</sup> Department of Mechanical Engineering, University of Cincinnati, Cincinnati, OH 45221-0072, USA

<sup>d</sup> Shanghai Institute of Applied Mathematics and Mechanics, Shanghai University, Shanghai 200072, PR China

### ARTICLE INFO

#### Article history:

Received 5 January 2010

Accepted 31 May 2010

Available online 21 August 2010

#### Keywords:

Boundary element method

Fast multipole method

Viscoelasticity

Multi-inclusion composite

### ABSTRACT

A fast multipole formulation for 2D linear viscoelastic problems is presented in this paper by incorporating the elastic–viscoelastic correspondence principle. Systems of multipole expansion equations are formed and solved analytically in Laplace transform domain. Three commonly used viscoelastic models are introduced to characterize the time-dependent behavior of the materials. Since the transformed multipole formulations are identical to those for the 2D elastic problems, it is quite easy to implement the 2D viscoelastic fast multipole boundary element method. Besides, all the integrals are evaluated analytically, leading to highly accurate results and fast convergence of the numerical scheme. Several numerical examples, including planar viscoelastic composites with single inclusion or randomly distributed multi-inclusions, as well as the problem of a crack in a pressured viscoelastic plane, are presented. The results are verified by comparison with the developed analytical solutions to illustrate the accuracy and efficiency of the approach.

© 2010 Elsevier Ltd. All rights reserved.

### 1. Introduction

It has long been accepted that most engineering materials exhibit noticeable time-effects, such as polymers, composites, non-ferrous metals, rocks, concrete and so on. Because of this time-effect, actual materials will possess viscous and elastic properties simultaneously and these properties will make many structures suffer from creep, relaxation and hysteresis problems. Therefore, it is crucial to fully understand the mechanism and response of viscoelastic materials under external loadings, so as to provide the scientific basis for predicting the service-life of the engineering components. Numerical techniques such as the boundary element method (BEM) are a promising tool in serving these purposes.

BEM can be regarded as a feasible numerical method, which is more accurate than finite element method (FEM) and other numerical methods, due to its features of dimensionality reduction for linear problems and high accuracy. Many investigators have applied the BEM to the investigation of viscoelastic characteristics of the materials. The most commonly used approach is the Laplace transform method [1–4]. By the elastic–viscoelastic correspondence principle [5], the viscoelastic governing equations can be transformed into a set of corresponding

elastic governing equations using the Laplace transform, and then the solutions are transformed back to the time domain by numerical methods. From the basic assumptions of viscoelastic constitutive relations and weighted residual techniques, Mesquita et al. [6–9] presented a boundary element alternative procedure for Boltzmann and Kelvin viscoelasticity. They produced the differential systems of equations with respect to time variable, which are solved by an appropriate time marching process. Combining the approach based on the two dimensional version of Somigliana's formula with the time-marching procedure described for the viscoelastic analysis by Mesquita et al., Huang et al. [10] considered the problem of an infinite, isotropic viscoelastic plane containing randomly distributed elastic inclusions. Sensale et al. [11–13] transformed the domain integral into a boundary integral using the dual reciprocity method for the stress analysis of bodies with aging viscoelastic constitutive relations. Birgisson et al. [14–16] applied a special boundary element-based method, called the displacement discontinuity method, and employed an explicit time-marching scheme to model the quasi-static responses of linear viscoelastic materials.

Analysis of viscoelastic problems often requires multi-time-step computation that can accurately predict the creep or relaxation behavior of the bodies under external loadings. Therefore, when we are dealing with large-scale models, such as the multi-inclusion composites, the computation time and storage space will increase significantly. The conventional boundary element-based method requires  $O(N^2)$  operations using iterative solvers (with  $N$  being the number of equations) because of its

\* Corresponding author. Tel.: +86 571 88208702; fax: +86 571 87952165.

E-mail addresses: zhuxingyi66@yahoo.com.cn (X.Y. Zhu),  
hzy@zju.edu.cn (Z.Y. Huang).

dense and non-symmetrical matrices. Thus conventional BEM-based approach is not suitable for solving viscoelastic problems with large-scale models. Fast multipole method (FMM) is a new algorithm developed recently for numerical solution of BEM. This algorithm has been proved that it can solve system of equations formed by BEM with higher efficiency and lower storage than that of the traditional solvers. Rokhlin and Greengard [17] first introduced the concept of fast multipole method to deal with 2D potential problems, and reduced the CPU time and memory usage in the fast multipole accelerated BEM to  $O(N)$ . The advantages of fast multipole BEM for large-scale problems make it considerably applicable for more practical applications.

For elasticity problems, many investigations have been carried out based on fast multipole BEM approaches. Greengard et al. [18,19] developed a fast multipole formulation for directly solving the biharmonic equations using Sherman's complex variables formulae. Peirce and Napier [20] gave a spectral multipole approach similar to the FMMs, reducing the complexities of both memory and operation to  $O(N \log N)$ . Yao et al. [21] and Wang et al. [22] presented a fast and accurate algorithm for modeling composite materials and crack problems. They applied complex Taylor expansion and adaptive tree structure to obtain a new shift of multipole expansion for two dimensional elastostatics. Liu et al. [23–25] proposed compact and efficient fast multipole BEM formulations for both 2D and 3D elasticity problems. In Liu's approach for 2D elastostatics [24], the displacement and traction kernels are represented using two complex analytic functions, and the two functions are first re-grouped and then expanded to form two moments for each kernel. This approach has recently been extended to 2-D multi-domain elasticity problems [26]. More information about the fast multipole BEM can be found in Ref. [27].

In this paper, a new fast multipole BEM for 2D viscoelastic problems is formulated. The elasticity version suggested by Liu [24] is extended to 2D viscoelastic multi-domain problems by virtue of the elastic–viscoelastic correspondence principle. Systems of the multipole expansion equations are formed in Laplace transform domain and solved by time step scheme. Three commonly used viscoelastic models are introduced to characterize the time-dependent behavior of the materials. Some practically important problems, such as the randomly distributed multi-inclusion planar viscoelastic composites and a pressured viscoelastic plane containing a crack are considered. Numerical results are presented and verified by the analytical solutions to further illustrate the accuracy and efficiency of the approach. It indicates that the method is not only easy in the meshing of complicated geometries, accurate for solving singular fields, but also practical and often superior in solving large-scale problems.

**2. FMBEM for 2D viscoelastic problems**

The boundary integral equation for isotropic, linearly viscoelastic materials in the time domain can be written as [28]

$$C_{ij}(\mathbf{x})u_j(\mathbf{x},t) = \int_S [U_{ij}(\mathbf{x},\mathbf{y},0)p_j(\mathbf{y},t) + \int_0^t p_j(\mathbf{y},t-\tau) \frac{\partial U_{ij}(\mathbf{x},\mathbf{y},\tau)}{\partial \tau} d\tau] dS(\mathbf{y}) - \int_S [P_{ij}(\mathbf{x},\mathbf{y},0)u_j(\mathbf{y},t) + \int_0^t u_j(\mathbf{y},t-\tau) \frac{\partial P_{ij}(\mathbf{x},\mathbf{y},\tau)}{\partial \tau} d\tau] dS(\mathbf{y}) \tag{1}$$

where  $C_{ij}(\mathbf{x})$  is a free term determined from the shape of the boundary at point  $\mathbf{x}$ ;  $u_i$  and  $p_i$  are the displacement and traction, respectively;  $U_{ij}$  and  $P_{ij}$  are the fundamental solutions of an infinite 2D viscoelastic plane. To solve Eq. (1), a time marching

scheme can be used. For example, according to the trapezoidal rule, Eq. (1) can be rewritten as follows:

$$C_{ij}(\mathbf{x})u_j(\mathbf{x},nh) = \int_S [U_{ij}(\mathbf{x},\mathbf{y},0)p_j(\mathbf{y},nh) + \frac{h}{2}p_j(\mathbf{y},nh)\hat{U}_{ij}(\mathbf{x},\mathbf{y},0)] dS(\mathbf{y}) - \int_S [P_{ij}(\mathbf{x},\mathbf{y},0)u_j(\mathbf{y},nh) + \frac{h}{2}u_j(\mathbf{y},nh)\hat{P}_{ij}(\mathbf{x},\mathbf{y},0)] dS(\mathbf{y}) + R_i^*[(n-1)h] \tag{2}$$

where  $\hat{U}_{ij}(\mathbf{x},\mathbf{y},t) = \partial U_{ij}(\mathbf{x},\mathbf{y},t)/\partial t$  and  $\hat{P}_{ij}(\mathbf{x},\mathbf{y},t) = \partial P_{ij}(\mathbf{x},\mathbf{y},t)/\partial t$ ,  $t = nh$  means the total time length  $t$  is divided into  $n$  time steps, and  $h$  is constant stepsize.  $R_i^*[(n-1)h]$  is the entire history when time  $t < nh$ , which can be written as

$$R_i^*[(n-1)h] = \frac{h}{2} \int_S \hat{U}_{ij}(\mathbf{x},\mathbf{y},h)p_j(\mathbf{y},0) dS(\mathbf{y}) - \frac{h}{2} \int_S \hat{P}_{ij}(\mathbf{x},\mathbf{y},h)u_j(\mathbf{y},0) dS(\mathbf{y}) (n = 1) \tag{3}$$

$$R_i^*[(n-1)h] = h \int_S \sum_{m=1}^{n-1} \hat{U}_{ij}(\mathbf{x},\mathbf{y},mh)p_j(\mathbf{y},[n-m]h) dS(\mathbf{y}) - h \int_S \sum_{m=1}^{n-1} \hat{P}_{ij}(\mathbf{x},\mathbf{y},mh)u_j(\mathbf{y},[n-m]h) dS(\mathbf{y}) + \frac{h}{2} \int_S \hat{U}_{ij}(\mathbf{x},\mathbf{y},h)p_j(\mathbf{y},0) dS(\mathbf{y}) - \frac{h}{2} \int_S \hat{P}_{ij}(\mathbf{x},\mathbf{y},h)u_j(\mathbf{y},0) dS(\mathbf{y}) (n = 2,3,\dots,N) \tag{4}$$

To solve Eq. (2), we should first know the fundamental solutions of the 2D viscoelastic problem. It is known that the governing equation of the viscoelastic problem is quite similar to that for the elastic problem when it is Laplace transformed [29]. Therefore we can obtain the fundamental solutions  $U_{ij}$  and  $P_{ij}$  by the elastic–viscoelastic correspondence principle. If the system is subjected to a Heaviside unit step force, the transformed viscoelastic fundamental solutions  $\tilde{U}_{ij}$  and  $\tilde{P}_{ij}$  can be defined in the Laplace domain as

$$\tilde{U}_{ij}(\mathbf{x},\mathbf{y},s) = \frac{1}{8\pi} \left[ \tilde{J}_1(s)\delta_{ij} \log\left(\frac{1}{r}\right) + \tilde{J}_2(s) \left( r_i r_j - \frac{1}{2} \delta_{ij} \right) \right] \tag{5}$$

$$\tilde{P}_{ij}(\mathbf{x},\mathbf{y},s) = \frac{1}{8\pi r} \left\{ \tilde{J}_3(s) \left( r_i n_j - r_j n_i - \frac{\partial r}{\partial n} \delta_{ij} \right) + \tilde{J}_4(s) \left[ \frac{\partial r}{\partial n} (\delta_{ij} - 4r_i r_j) + r_j n_i - r_i n_j \right] \right\} \tag{6}$$

In the viscoelastic analysis, for many cases it can be assumed that the material behaves elastically in dilatation. Thus the bulk modulus  $K$  is a constant, while the viscoelastic shear modulus  $G$  and the Poisson's ratio  $\nu$  are time-dependent in general. This assumption is made for simplicity and could reduce the complexity of the mathematical derivations. In such a case, the functions  $\tilde{J}_1(s), \tilde{J}_2(s), \tilde{J}_3(s), \tilde{J}_4(s)$  appearing in Eqs. (5) and (6) can be obtained as

$$\tilde{J}_1(s) = \frac{2(3K + 7\tilde{G})}{\tilde{G}(3K + 4\tilde{G})s} \tag{7}$$

$$\tilde{J}_2(s) = \frac{2(3K + \tilde{G})}{\tilde{G}(3K + 4\tilde{G})s} \tag{8}$$

$$\tilde{J}_3(s) = \frac{2(3K + 7\tilde{G})}{(3K + 4\tilde{G})s} \tag{9}$$

$$\tilde{J}_4(s) = \frac{2(3K + \tilde{G})}{(3K + 4\tilde{G})s} \quad (10)$$

with  $s$  being the transform parameter. Notice that the constitutive equations for a linear viscoelastic material in the differential form are:

$$\begin{aligned} P'S_{ij} &= Q'e_{ij} \\ \tilde{G} &= \frac{Q'(s)}{2P'(s)} \end{aligned} \quad (11)$$

where  $P', Q'$  are time differential operators and  $S_{ij}, e_{ij}$  are the deviator components of the stress and strain tensors. Then, Eqs. (7)–(10) can accordingly be expressed as

$$\tilde{J}_1(s) = \frac{2P'(s)[6KP'(s) + 7Q'(s)]}{sQ'(s)[3KP'(s) + 2Q'(s)]} \quad (12)$$

$$\tilde{J}_2(s) = \frac{2P'(s)[6KP'(s) + Q'(s)]}{sQ'(s)[3KP'(s) + 2Q'(s)]} \quad (13)$$

$$\tilde{J}_3(s) = \frac{6KP'(s) + 7Q'(s)}{s[3KP'(s) + 2Q'(s)]} \quad (14)$$

$$\tilde{J}_4(s) = \frac{6KP'(s) + Q'(s)}{s[3KP'(s) + 2Q'(s)]} \quad (15)$$

By applying Laplace inverse transform to Eqs. (5) and (6), it is readily easy to obtain the viscoelastic fundamental solutions in the time domain.

Based on Eqs. (5) and (6), we can further establish the multipole expansion formulations of the 2D viscoelastic problem. Assume that  $p_j$  and  $u_j$  are piecewisely constant over each of the  $N$  intervals constituting the boundary  $S$ . Similar to the multipole expansion formulations developed by Liu [24], the integral equations in Eq. (2) can be written in complex forms as follows:

$$\begin{aligned} D_p(z_0, t, \tau) &= \int_{S_0} U_{ij}(\mathbf{x}, \mathbf{y}, \tau) p_j(\mathbf{y}, t) dS(\mathbf{y}) \\ &= \frac{1}{16\pi} \int_{S_0} \left\{ J_1(\tau) Ge(z_0, z) p(z, t) - J_2(\tau) z_0 \overline{Ge'(z_0, z)} \overline{p(z, t)} \right. \\ &\quad \left. + J_2(\tau) z \overline{Ge'(z_0, z)} \overline{p(z, t)} + J_1(\tau) \overline{Ge(z_0, z)} p(z, t) \right\} dS(z) \end{aligned} \quad (16)$$

$$\begin{aligned} D_u(z_0, t, \tau) &= \int_{S_0} P_{ij}(\mathbf{x}, \mathbf{y}, \tau) u_j(\mathbf{y}, t) dS(\mathbf{y}) \\ &= -\frac{1}{8\pi} \int_{S_0} \left\{ J_3(\tau) Ge'(z_0, z) n(z) u(z, t) \right. \\ &\quad \left. - J_4(\tau) z_0 \overline{Ge''(z_0, z)} \overline{n(z) u(z, t)} + J_4(\tau) z \overline{Ge''(z_0, z)} \overline{n(z) u(z, t)} \right. \\ &\quad \left. + J_4(\tau) \overline{Ge'(z_0, z)} [n(z) \overline{u(z, t)} + \overline{n(z)} u(z, t)] \right\} dS(z) \end{aligned} \quad (17)$$

where  $J_1(t), J_2(t), J_3(t), J_4(t)$  are inverted from Eqs. (12)–(15),

$$\begin{aligned} J_1(t) &= L^{-1}[\tilde{J}_1(s)], \quad J_2(t) = L^{-1}[\tilde{J}_2(s)] \\ J_3(t) &= L^{-1}[\tilde{J}_3(s)], \quad J_4(t) = L^{-1}[\tilde{J}_4(s)] \end{aligned} \quad (18)$$

Rearranging Eqs. (16) and (17), one obtains

$$\begin{aligned} D_p(z_0, t, \tau) &= \frac{1}{16\pi} \left[ \sum_{k=0}^{\infty} O_k(z_0 - z_c) R_k(z_c, t, \tau) \right. \\ &\quad \left. + z_0 \sum_{k=0}^{\infty} \overline{O_{k+1}(z_0 - z_c)} A_k(z_c, t, \tau) \right. \\ &\quad \left. + \sum_{k=0}^{\infty} \overline{O_k(z_0 - z_c)} W_k(z_c, t, \tau) \right] \end{aligned} \quad (19)$$

$$\begin{aligned} D_u(z_0, t, \tau) &= \frac{1}{8\pi} \left[ \sum_{k=1}^{\infty} O_k(z_0 - z_c) Y_k(z_c, t, \tau) \right. \\ &\quad \left. + z_0 \sum_{k=0}^{\infty} \overline{O_{k+1}(z_0 - z_c)} B_k(z_c, t, \tau) \right. \\ &\quad \left. + \sum_{k=0}^{\infty} \overline{O_k(z_0 - z_c)} V_k(z_c, t, \tau) \right] \end{aligned} \quad (20)$$

where  $R_k, A_k, W_k, Y_k, B_k,$  and  $V_k$  are called moments about  $z_c$  which are independent of the collocation point  $z_0$  and only need to be computed once. They are evaluated as follows:

$$R_k(z_c, t, \tau) = J_1(\tau) \int_{S_0} I_k(z - z_c) p(z, t) dS(z) \quad (k \geq 0) \quad (21)$$

$$A_k(z_c, t, \tau) = J_2(\tau) \int_{S_0} I_k(z - z_c) p(z, t) dS(z) \quad (k \geq 0) \quad (22)$$

$$\begin{aligned} W_k(z_c, t, \tau) &= J_1(\tau) \int_{S_0} \overline{I_k(z - z_c)} p(z, t) dS(z) \\ &\quad - J_2(\tau) \int_{S_0} \overline{I_{k-1}(z - z_c)} z \overline{p(z, t)} dS(z) \quad (k \geq 1) \end{aligned} \quad (23)$$

$$W_0(z_c, t, \tau) = J_1(\tau) \int_{S_0} p(z, t) dS(z) \quad (24)$$

$$Y_k(z_c, t, \tau) = J_3(\tau) \int_{S_0} I_{k-1}(z - z_c) n(z) u(z, t) dS(z) \quad (k \geq 1) \quad (25)$$

$$B_k(z_c, t, \tau) = J_4(\tau) \int_{S_0} I_{k-1}(z - z_c) n(z) u(z, t) dS(z) \quad (26)$$

$$\begin{aligned} V_k(z_c, t, \tau) &= \int_{S_0} J_4(\tau) \left\{ \overline{I_{k-1}(z - z_c)} [n(z) \overline{u(z, t)} + \overline{n(z)} u(z, t)] \right. \\ &\quad \left. - \overline{I_{k-2}(z - z_c)} z \overline{n(z) u(z, t)} \right\} dS(z) \quad (k \geq 2) \end{aligned} \quad (27)$$

$$V_1(z_c, t, \tau) = J_4(\tau) \int_{S_0} [n(z) \overline{u(z, t)} + \overline{n(z)} u(z, t)] dS(z) \quad (28)$$

in which,  $O_k$  and  $I_k$  are two auxiliary functions:

$$I_k = \frac{z^k}{k!} \quad \text{for } k \geq 0 \quad (29)$$

$$O_0(z) = -\ln(z), \quad O_k(z) = \frac{(k-1)!}{z^k} \quad \text{for } k \geq 1 \quad (30)$$

It should be mentioned that we can obtain the results of displacements and tractions at  $t=0$  by the conventional FMBEM for pure elasticity. Then, the multipole expansion for the viscoelastic problem can be easily formulated step by step. It is also understandable that the M2M, M2L and L2L translations remain the same as that for the elastostatic problems. Thus, it is not difficult to program the new 2D viscoelastic counterpart based on the fast multipole BEM code for the 2D elastic problems. Detailed analysis and formulations of the subsequent multipole translations and implementations of FMM can be found in Ref. [24], for example.

### 3. Linear viscoelastic models

The viscoelastic materials exhibit both elastic and viscous properties simultaneously under appropriate conditions, and then accordingly possess creep, relaxation or hysteresis phenomena. To describe this kind of materials approximately, we can combine

spring and dashpot elements in series, in parallel or in a more complicated way. Here we choose three types of models to represent the linear viscoelastic behavior of the real materials. Fig. 1(a) shows the Voigt–Kelvin model, which can describe a body that has delayed elasticity. However, it cannot describe the relaxation phenomenon. Fig. 1(b) shows the Burgers model which describes a body that has instantaneous elasticity, delayed elasticity and viscous flow. It can also be used to simulate the materials working under high stress or high temperature. Fig. 1(c) presents the two Voigt+one spring model which is commonly used, because it can fit experimental curves better. Thus, we often use it to describe the viscoelastic solids in engineering, such as concrete and rock. The operators  $P'(s)$ ,  $Q'(s)$  for the three types can be written as follows, respectively:

$$P'(s) = 1, \quad Q'(s) = E + \eta s \tag{31}$$

$$P'(s) = 1 + \left( \frac{\eta_1}{E_1} + \frac{\eta_1 + \eta_2}{E_2} \right) s + \frac{\eta_1 \eta_2}{E_1 E_2} s^2, \quad Q'(s) = \eta_1 s + \frac{\eta_1 \eta_2}{E_2} s^2 \tag{32}$$

$$P'(s) = 1 + \frac{E_1 \eta_2 + E_2 \eta_1 + E_0 \eta_1 + E_0 \eta_2}{E_1 E_2 + E_1 E_0 + E_0 E_2} s + \frac{\eta_1 \eta_2}{E_1 E_2 + E_1 E_0 + E_0 E_2} s^2$$

$$Q'(s) = \frac{E_0 E_1 E_2}{E_1 E_2 + E_1 E_0 + E_0 E_2} + \frac{E_0 E_1 \eta_2 + E_0 E_2 \eta_1}{E_1 E_2 + E_1 E_0 + E_0 E_2} s + \frac{E_0 \eta_1 \eta_2}{E_1 E_2 + E_1 E_0 + E_0 E_2} s^2 \tag{33}$$

Once we choose the model to describe the linear viscoelastic behavior, then following the procedure presented in Section 2, we can get the fundamental solution for the viscoelastic problem. As an example, we present four basic time functions for the Voigt–Kelvin type materials:

$$J_1(t) = -\frac{4}{E} \exp\left(-\frac{Et}{\eta}\right) - \frac{2}{E(3-4\nu)} \left\{ (3-6\nu) \exp\left[\frac{E(3-4\nu)t}{2\eta(2\nu-1)}\right] - 9 + 14\nu \right\} \tag{34}$$

$$J_2(t) = -\frac{4}{E} \exp\left(-\frac{Et}{\eta}\right) + \frac{2}{E(3-4\nu)} \left\{ (3-6\nu) \exp\left[\frac{E(3-4\nu)t}{2\eta(2\nu-1)}\right] + 3 - 2\nu \right\} \tag{35}$$

$$J_3(t) = \frac{3}{6-8\nu} \exp\left[\frac{E(3-4\nu)t}{2\eta(2\nu-1)}\right] + \frac{9-14\nu}{3-4\nu} \tag{36}$$

$$J_4(t) = -\frac{3}{6-8\nu} \exp\left[\frac{E(3-4\nu)t}{2\eta(2\nu-1)}\right] + \frac{3-2\nu}{3-4\nu} \tag{37}$$

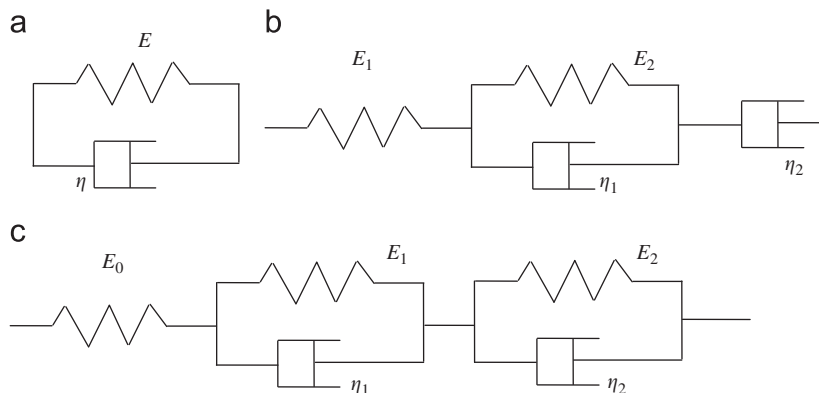


Fig. 1. Three models representing the linear viscoelastic behavior.

### 4. Numerical examples

We consider in this section several examples to verify the proposed numerical procedures of the fast multipole BEM for 2D multi-domain viscoelastic problems. The analytical solutions are also developed here to compare with the numerical results. As we mentioned before, the multipole expansion formulations given in our work closely follows the ideas in [24] which basically invokes the FMM for Laplace’s equation, therefore it will lead to an  $O(N)$  numerical method in problems with  $N$  unknowns. However, since  $R_i^*$  appears in Eq.(2) which involves the entire history up to time  $t < nh$ , comparing to the previous time step, the next time step will cost more CPU time.

#### 4.1. A simple concentric cylinder

We first study a simple concentric cylinder to verify the BEM program for multi-domain problems, Fig. 2. In this case, a solid cylindrical fiber is embedded in a larger matrix, where the matrix is isotropic, linear viscoelastic material, which is modeled by the Burgers type model, and the fiber is isotropic elastic. Applying the theory of elasticity for plane strain case in the polar coordinate system, one can derive the following expressions for the radial displacement and stress fields in the fiber and matrix, respectively:

$$u_r^f = A_f r, \quad 0 \leq r \leq a \tag{38}$$

$$u_r^m = A_m r + \frac{B_m}{r}, \quad a \leq r \leq b \tag{39}$$

$$\sigma_r^f = \frac{A_f E_f}{(1+\nu_f)(1-2\nu_f)}, \quad 0 \leq r \leq a \tag{40}$$

$$\sigma_r^m = \frac{E_m}{(1+\nu_m)(1-2\nu_m)} \left( A_m - \frac{B_m}{r^2} + 2\nu_m \frac{B_m}{r^2} \right), \quad a \leq r \leq b \tag{41}$$

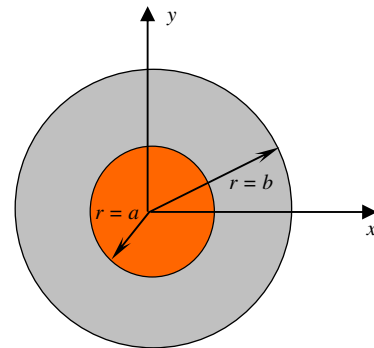


Fig. 2. A concentric cylinder.

Here it is assumed that a radial displacement  $\delta$  or a radial tension  $\delta$  is prescribed on the outer boundary of the matrix  $r=b$ . Thus the boundary and interface conditions are:

$$r = b : u_r^m = \delta \text{ (condition 1) or } \sigma_r^m = \delta \text{ (condition 2)} \quad (42)$$

$$r = a : u_r^m = u_r^f, \quad \sigma_r^m = \sigma_r^f \quad (43)$$

Three constants  $A_f$ ,  $A_m$  and  $B_m$  can be solved by combining Eqs.(38)–(43):

$$\begin{aligned} A_m &= \frac{\delta b(1-2\nu_m + \alpha)}{a^2 + b^2 - 2\nu_m b^2 + \alpha(b^2 - a^2)} \\ A_f &= \frac{2\delta b(1-\nu_m)}{a^2 + b^2 - 2\nu_m b^2 + \alpha(b^2 - a^2)} \\ B_m &= \frac{\delta b a^2(1-\alpha)}{a^2 + b^2 - 2\nu_m b^2 + \alpha(b^2 - a^2)} \end{aligned} \quad (44)$$

for condition 1, and

$$\begin{aligned} A_m &= \frac{\delta b^2 \beta(2\nu_m - 1 - \alpha)}{(b^2 - a^2)(2\nu_m - 1) + \alpha(2a^2\nu_m - a^2 - b^2)} \\ B_m &= \frac{\delta a^2 b^2 \beta(\alpha - 1)}{(b^2 - a^2)(2\nu_m - 1) + \alpha(2a^2\nu_m - a^2 - b^2)} \end{aligned}$$

$$A_f = \frac{2\delta b^2 \beta(\nu_m - 1)}{(b^2 - a^2)(2\nu_m - 1) + \alpha(2a^2\nu_m - a^2 - b^2)} \quad (45)$$

for condition 2, and

$$\alpha = \frac{E_f(1 + \nu_m)(1 - 2\nu_m)}{E_m(1 + \nu_f)(1 - 2\nu_f)}, \quad \beta = \frac{(1 + \nu_m)(1 - 2\nu_m)}{E_m} \quad (46)$$

The effective elastic material properties can be directly converted to the viscoelastic properties by using the correspondence principle on the basis of Laplace transform. The correspondence process is performed by replacing each elastic modulus with the corresponding modulus related to time. It should be mentioned again that the elastic modulus of the rigid inclusion and bulk modulus of each phase are assumed constant. For example, the radial displacements in Laplace transform domain at  $r=a$  under condition 2 can be written as

$$\begin{aligned} \tilde{u}_{ra}(s) &= \frac{\delta a b^2 \tilde{\beta}(2\tilde{\nu}_m - 1 - \tilde{\alpha})}{s[(b^2 - a^2)(2\tilde{\nu}_m - 1) + \tilde{\alpha}(2a^2\tilde{\nu}_m - a^2 - b^2)]} \\ \tilde{\alpha} &= \frac{E_f(1 + \tilde{\nu}_m)(1 - 2\tilde{\nu}_m)}{\tilde{E}_m(1 + \nu_f)(1 - 2\nu_f)}, \quad \tilde{\beta} = \frac{(1 + \tilde{\nu}_m)(1 - 2\tilde{\nu}_m)}{\tilde{E}_m} \\ \tilde{E}_m &= \frac{9\tilde{G}_m K_m}{(3K_m + \tilde{G}_m)}, \quad \tilde{\nu}_m = \frac{3K_m - 2\tilde{G}_m}{2(3K_m + \tilde{G}_m)}, \quad \tilde{G}_m = \frac{Q'(s)}{2P'(s)} \end{aligned} \quad (47)$$

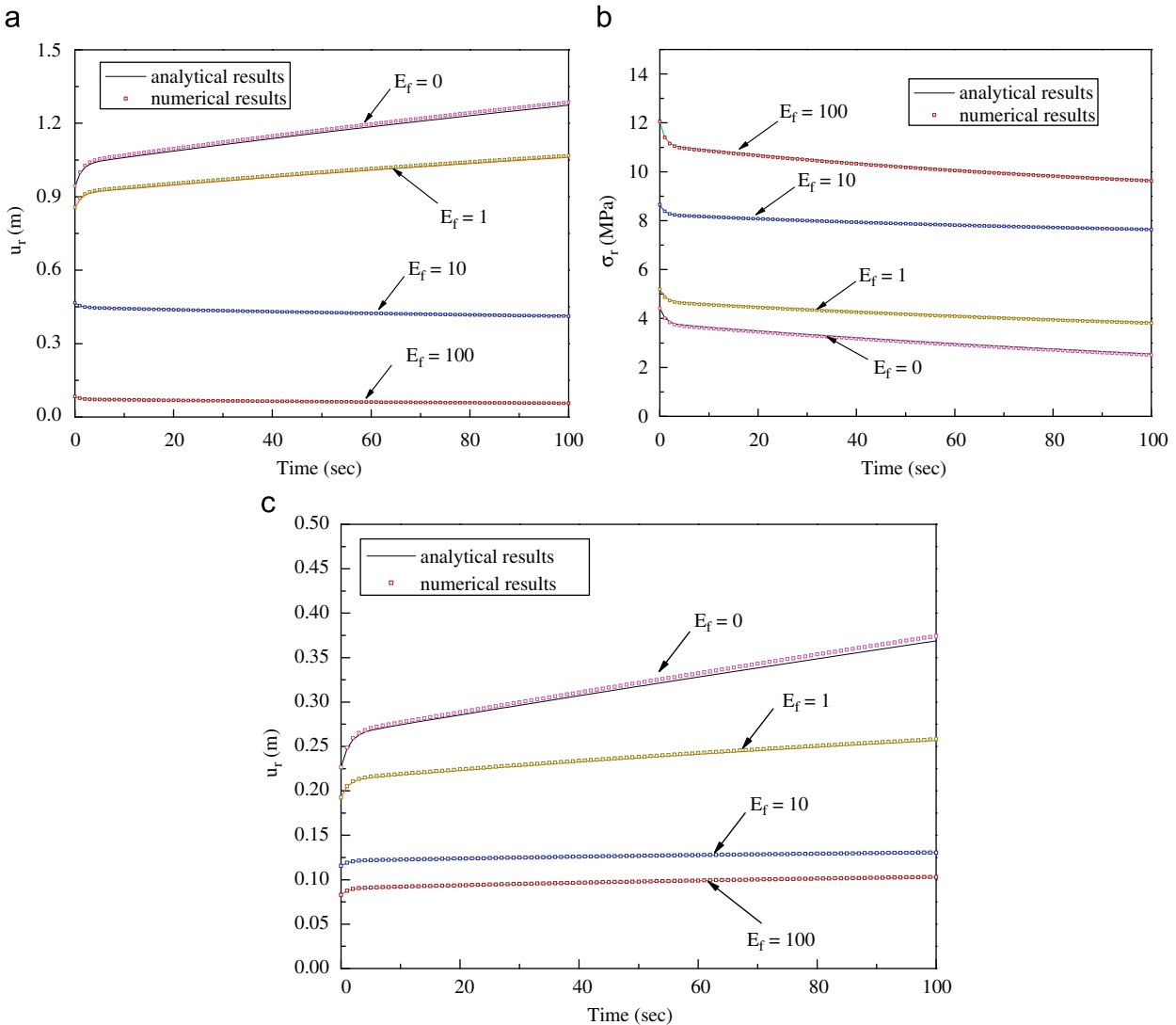


Fig. 3. Comparison of analytical and numerical results of (a) displacement (condition 1 at  $r=a$ ); (b) stress (condition 1 at  $r=a$ ); (c) displacement (condition 2 at  $r=b$ ).

In the numerical calculation, the following material parameters for the matrix are used:

$$\begin{aligned} \text{for matrix } E_1 &= 10\text{MPa}, E_2 = 25\text{MPa} \\ \eta_1 &= 750\text{MPa} \cdot \text{s}, \eta_2 = 35\text{MPa} \cdot \text{s} \end{aligned} \quad (48)$$

The numerical results are obtained by using 200 elements on the outer boundary and 200 elements on the interface. Fig. 3 plots the variations with time of the radial displacement and stress at  $r=a$  or  $r=b$  under condition 1 or condition 2. The numerical results calculated by the fast multipole BEM are compared with the exact analytical solution presented above. Four different values of Young’s modulus of the fiber ( $E_f=0, 1, 10$  and  $100$ ) have been considered. It is shown that the FMBEM simulation results are in excellent agreement with the analytical solution, which indicates that the developed fast multipole BEM is adequate to predict the viscoelastic behavior of multi-inclusion composites. It should be mentioned that this example is identical to the thick-walled hollow cylinder subjected to an external pressure case when  $E_f=0$ . It is interesting from the results that the radial displacement at  $r=a$  increases with the increase of the time when the Young’s modulus of the fiber is relatively low, while the displacement decreases with the time when the Young’s modulus of the fiber is relatively high, see Fig. 3(a).

#### 4.2. A crack in a pressured viscoelastic plane

We next study the accuracy of the fast multipole BEM for a crack-like inclusion in a viscoelastic plane of the Voigt–Kelvin type. Since we employ constant boundary elements to discretize the BIE, all integrals can be evaluated analytically, which make it easy to deal with the nearly singular integrations problems. The crack is modeled by an elliptical hole in FMBEM simulation, with the length of the crack  $b=0.025$ , and  $a/b=0.01$ . The crack is located at the center of a square sheet which is subjected to a unit uniform and uniaxial tension  $P$  in the  $x$ -direction, as depicted in Fig. 4.

When  $a/b=0$ , according to the fracture mechanics [30], the crack opening displacement  $u(x, t)$  for the viscoelastic problem can be evaluated as

$$\begin{aligned} u(x, t) &= \frac{p\sqrt{b^2-x^2}}{(6K+E)E} \left\{ -\exp\left(-\frac{Et}{\eta}\right)(6K+E) + 6K \right. \\ &\quad \left. + E \left[ 4 - 3\exp\left(-\frac{(6K+E)t}{\eta}\right) \right] \right\} \end{aligned} \quad (49)$$

where  $E$  is the spring constant and  $\eta$  is the viscosity coefficient of the dashpot as illustrated in Fig.1(a). The following Voigt–Kelvin model parameters are used:

$$\text{for matrix } E = 23500 \text{ MPa}, \eta_1 = 425 \text{ MPa} \cdot \text{s}, K = 15666.6667 \text{ MPa} \quad (50)$$

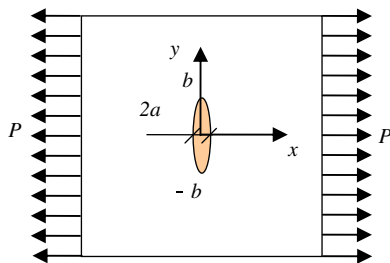


Fig. 4. Viscoelastic plane containing a crack-like inclusion.

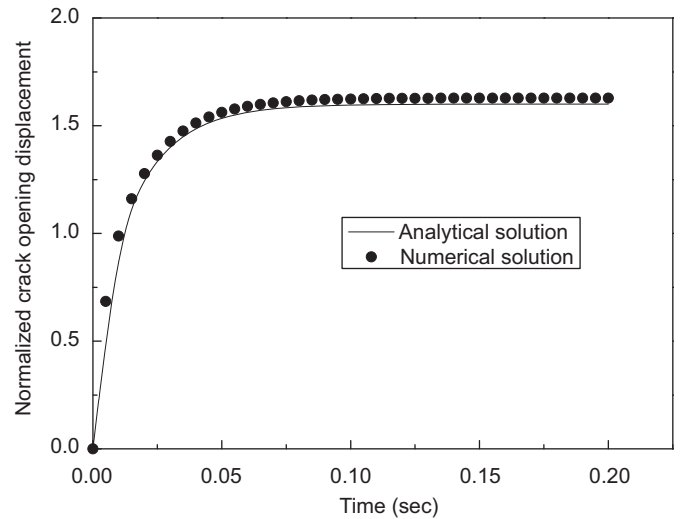


Fig. 5. Normalized crack opening displacement.

Fig. 5 presents the normalized crack opening displacement at the center of the crack ( $x=0$ ) calculated by the fast multipole BEM, which is compared with the analytical solution for the idealized crack  $a/b=0$ , where the normalized displacement  $\bar{u}(x, t)$  can be defined as

$$\bar{u}(x, t) = \frac{Ku(x, t)}{Pb} \quad (51)$$

It is seen that the results obtained from the FMBEM agree well with the corresponding analytical solutions. It should be mentioned that because of the characteristics of the Voigt–Kelvin model, the displacement at the center of the crack will reach a specific value when  $t$  tends to infinity.

#### 4.3. Multi-inclusion problems

In the last example, we study the properties of multi-phase planar viscoelastic composites (plane strain condition). The problem examined is that of randomly distributed circular elastic inclusions or holes embedded in a matrix possessing the linear viscoelastic properties, which is modeled by the two Voigt+one spring type model. First, we follow a popular micromechanical method, Mori–Tanaka method, to approximately determine the effective composite properties when the matrix is viscoelastic. This method has been widely applied for elastic phases, and can be extended to the viscoelastic case by the correspondence principle. Due to the isotropy of the overall stiffness tensor, the effective shear modulus  $G$  and planar bulk modulus  $K$  for the composite with circular inclusions, estimated by Mori–Tanaka method, are expressed as

$$G = G_0 \left[ 1 + \frac{2f}{(1-f)(K_0 + 2G_0)/(K_0 + G_0) + 2G_0/(G_1 - G_0)} \right] \quad (52)$$

$$K = K_0 \left[ 1 + \frac{f}{(1-f)K_0/(K_0 + G_0) + K_0/(K_1 - K_0)} \right] \quad (53)$$

where  $K_0$  and  $G_0$  are the shear modulus and bulk modulus of the matrix, and  $K_1$  and  $G_1$  are the shear modulus and bulk modulus for the inclusion, respectively, and  $f$  is the volume content of the inclusions. Based on the relationship between the elastic constants, the effective Young’s modulus of the composite can

be obtained quite easily for the two-dimensional case as

$$E = \frac{4GK}{K+G} \tag{54}$$

Using the same method and hypothesis as Example 1, the constitutive equation of the composite in the Laplace transform domain becomes

$$\varepsilon(s) = \frac{\bar{\sigma}}{s\tilde{E}} \tag{55}$$

where  $\bar{\sigma}$  is the uniaxial tension applied to the opposite edges,  $\varepsilon(s)$  is the average strain of the composite along the tension direction in the transform domain, and  $\tilde{E}$  is the effective Young's modulus of the composite in the Laplace transform domain, which can be expressed as

$$\begin{aligned} \tilde{E} &= \frac{4\tilde{G}\tilde{K}}{\tilde{K}+\tilde{G}} \\ \tilde{G} &= \tilde{G}_0 \left[ 1 + \frac{2f}{(1-f)(K_0+2\tilde{G}_0)/(K_0+\tilde{G}_0)+2\tilde{G}_0/(G_1-\tilde{G}_0)} \right] \\ \tilde{K} &= K_0 \left[ 1 + \frac{f}{(1-f)K_0/(K_0+\tilde{G}_0)+K_0/(K_1-K_0)} \right], \quad \tilde{G}_0 = \frac{Q'(s)}{2P'(s)} \end{aligned} \tag{56}$$

Applying the Laplace inverse transform to Eq. (55) from the transform domain into the time domain, one can obtain the time variation of the average strain of the composite along the tension direction.

For the multi-inclusion composite, analytical solution is obtained for the average strain, which can be employed to compare with the developed fast multipole BEM results. For calculation of the average strain along the tension direction by FMBEM, the sheet is subjected to a unit uniform and uniaxial tension in  $x$ -direction, see Fig. 6. It has been reported by Hu et al. [31] that the results tend to be stable when the number of inclusions is greater than 100, and then the body presents apparent homogeneous and isotropic characteristics. Therefore, in our example, the number of inclusions is kept to be 100, and the radius of inclusions is changed with the volume content of the fibers. Once all the boundary values are determined, one can use the results to estimate the average strain of materials with multi-inclusions. The average strain in the longitudinal direction is determined by

$$\bar{\varepsilon}_x = \frac{\bar{U}_{AB} + \bar{U}_{CD}}{L} \tag{57}$$

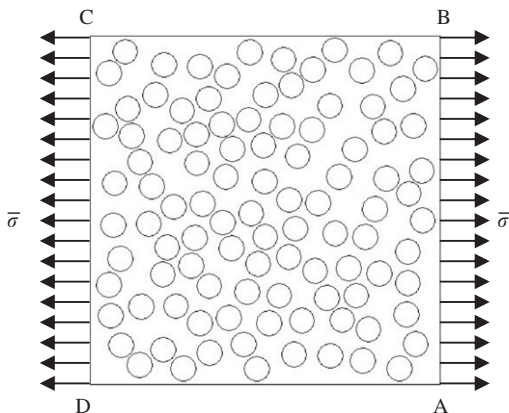


Fig. 6. Viscoelastic matrix embedded with elastic circular inclusions.

where  $L$  is the length of the square sheet, and  $\bar{U}$  is the effective displacement calculated from the fast multipole BEM results as

$$\bar{U} = \frac{\sum_e^n \int_{\Gamma_e} U_e d\Gamma_e}{L} \tag{58}$$

Creep problems are often encountered in civil engineering in many cases, such as pressure pipes and asphalt pavement. It is known that most engineering materials more or less have the viscoelastic characteristics, which will make many structures suffer from creep under some environmental conditions. Here, we also investigate the creep characteristics of the multi-inclusion composite from the numerical results:

$$J(t) = \frac{\bar{\varepsilon}_x}{\bar{\sigma}} \tag{59}$$

where  $J(t)$  is the creep compliance, which is defined as the strain function in time resulted from the application of a unit step stress. In linearly viscoelastic materials, the creep compliance is independent of stress level.

The analytical and numerical results for the average strain of the multi-inclusion composite are calculated with the following parameters:

for matrix  $E_0 = 1.926$  MPa,  $E_1 = 2.328$  MPa,  $E_2 = 1.389$  MPa

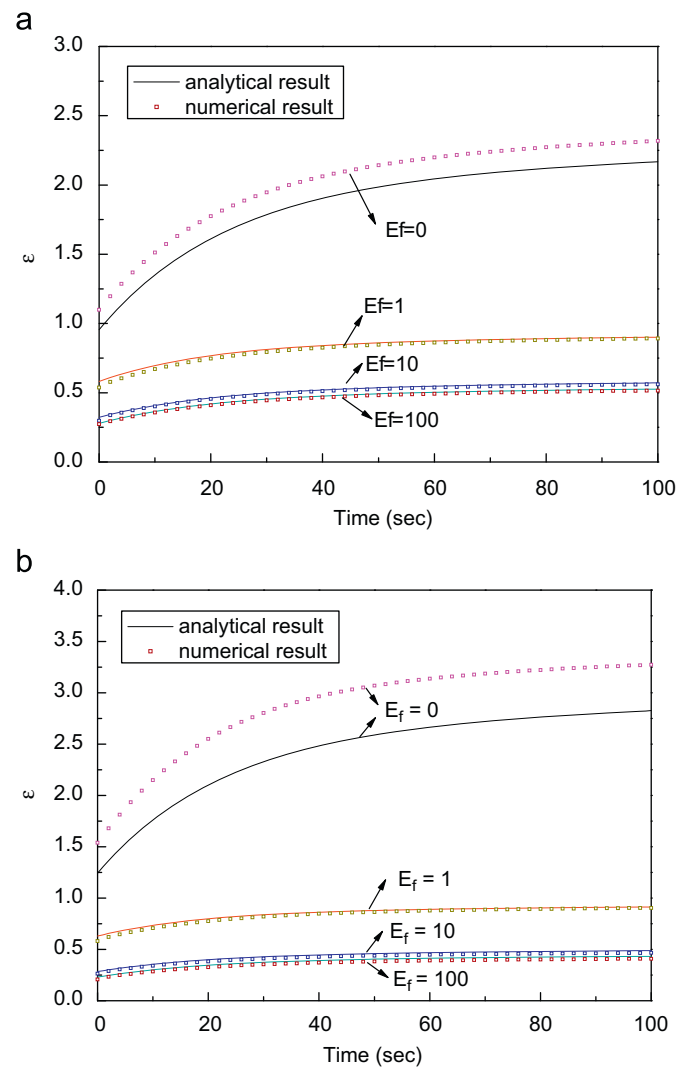


Fig. 7. Comparison of the numerical and analytical average strains for (a) volume fraction  $f=0.3$  and (b) volume fraction  $f=0.4$ .

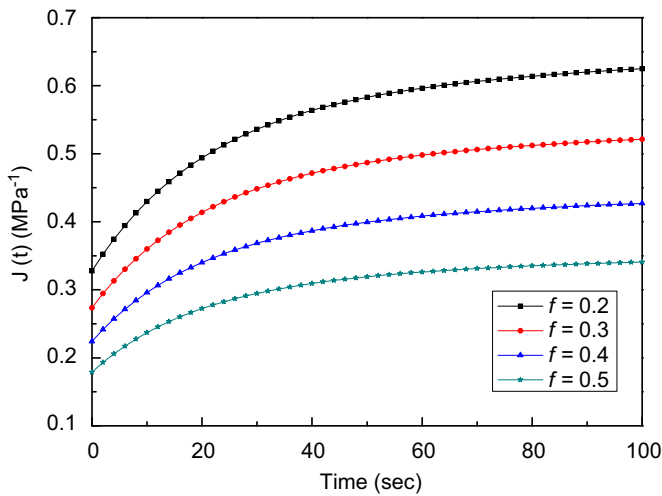


Fig. 8. The creep compliance curves for various volume fractions.

$$\eta_1 = 752.516 \text{ MPa} \cdot \text{s}, \quad \eta_2 = 31.549 \text{ MPa} \cdot \text{s}$$

for fiber  $v_f = 0.25$ ,  $E_f = 0 \sim 100 \text{ MPa}$  (60)

The numerical solution is obtained by using 200 elements on the outer boundary and 20 elements on each interface of the inclusions. Fig. 7 presents the time variation of the average strain along the  $x$ -direction when Young's modulus of the fibers  $E_f = 0, 1, 10$  and  $100$ . Both the analytical results predicted from the micromechanical model presented above and the numerical ones calculated by fast multipole BEM are given. It is noted that the fast multipole BEM simulation results again show good agreement with the analytical predictions, especially for multi-inclusion composites. However, for a viscoelastic plane with multiple circular holes, the numerical results are not quite close to the analytical prediction, but they show the same trend of changing with the time. This is quite reasonable, because for the case of holes, there are obvious differences in results obtained from various analytical approaches when the volume fraction of holes is high. For instance, it has been reported that the effective Young's modulus predicted by the Mori–Tanaka method is higher than the result of the generalized self-consistent method [31].

Fig. 8 shows the effect of the volume content on the creep compliance when multiple rigid inclusions ( $E_f = 10^8 \text{ MPa}$ ) are embedded in a viscoelastic matrix. During creep at a constant force, the strain increases with time. The corresponding creep compliance increases with the decrease of the volume content of the inclusions. This indicates that at a lower volume content, the material will creep faster.

## 5. Conclusions

A new approach for analyzing the time-dependent behavior of linear viscoelastic materials by the fast multipole BEM via the elastic–viscoelastic correspondence principle is presented. The transformed fast multipole formulations have been established and the inversions of the related transformed functions are performed analytically. Since the resulting M2M, M2L and L2L translations are identical to those for the 2D elastic case presented in Ref. [24], it is quite easy to program the 2D viscoelastic fast multipole BEM based on the counterpart for the 2D elastic case.

Several viscoelastic models are adopted to characterize the creep behavior of linear viscoelastic materials. In our paper, all the integrals are evaluated analytically, leading to highly accurate

results and fast convergence of the numerical scheme. Three numerical examples are given to demonstrate the accuracy, efficiency, and versatility of the developed fast multipole BEM for viscoelastic problems. It indicates that this method is not only easy in the meshing of complicated geometries, accurate for solving singular fields or fields in infinite domain, but also practical and often superior in solving large-scale problems. In general, the advantage of fast multipole BEM in higher speed and lower storage makes it possible to deal with many potential application problems, especially for multi-time-step problems (e.g. the viscoelastic case).

The extension of the present fast multipole BEM simulation and analytical study to 3D viscoelastic problems will be an interesting topic. Besides, consideration of interfacial cracking process of multi-inclusion viscoelastic composites under external loadings will be another challenge, which is very important for the exploration of failure mechanism of viscoelastic composites. Research results along these lines will be reported in future works.

## Acknowledgement

The work was sponsored by the National Natural Science Foundation of China (No. 10725210) and the National Basic Research Program of China (No. 2009CB623200).

## References

- [1] Rizzo FJ, Shippy DJ. An application of the correspondence principle of linear viscoelasticity theory. *SIAM J Appl Math* 1971;21:321–30.
- [2] Kusama T, Mitsui Y. Boundary element method applied to linear viscoelastic analysis. *Appl Math Modelling* 1982;6:285–94.
- [3] Sun BN, Hsiao CC. Viscoelastic boundary method for analysing polymer quasi fracture. *Comput Struct* 1988;30:963–6.
- [4] Liu Y, Antes H. Application of visco-elastic boundary element method to creep problems in chemical engineering structures. *Int J Pressure Vessels Piping* 1997;70:27–31.
- [5] Tschoegl NW. The phenomenological theory of linear viscoelastic behavior: an introduction. New York: Springer; 1989.
- [6] Mesquita AD, Coda HB, Venturini WS. An alternative time marching process for viscoelastic analysis by BEM and FEM. *Int J Numer Meth Eng* 2001;51:1157–73.
- [7] Mesquita AD, Coda HB. An alternative time integration procedure for Boltzmann viscoelasticity: a BEM approach. *Comput Struct* 2001;79/16:1487–96.
- [8] Mesquita AD, Coda HB. Boundary integral equation method for general viscoelastic analysis. *Int J Solids Struct* 2002;39:2643–64.
- [9] Mesquita AD, Coda HB. A simple Kelvin and Boltzmann viscoelastic analysis of three-dimensional solids by the boundary element method. *Eng Anal Bound Elem* 2003;27:885–95.
- [10] Huang Y, Crouch SL, Mogilevskaia SG. A time domain direct boundary integral method for a viscoelastic plane with circular holes and elastic inclusions. *Eng Anal Bound Elem* 2005;29:725–37.
- [11] Sensale B, Creus GJ. Boundary element analysis of viscoelastic fracture. In: *Boundary element XV*, vol. 2. Southampton: Computational Mechanics Publication; 1993. p. 291–302.
- [12] Sensale B. On the solution of viscoelastic problems using boundary elements techniques. DSc thesis, CEMACOM, UFRGS, Porto Alegre, Portuguese, 1997.
- [13] Sensale B, Partridge PW, Creus GJ. General boundary elements solution for aging viscoelastic structures. *Int J Numer Meth Eng* 2001;50:1455–68.
- [14] Birgisson B, Sangpetngam B, Roque R. Prediction of the viscoelastic response and crack growth in asphalt mixtures using the boundary element method. *Transp Res Rec* 2002;1789:129–35.
- [15] Birgisson B, Soranakom C, Napier JAL, Roque R. Microstructure and fracture in asphalt mixtures using a boundary element approach. *J Mater Civ Eng* 2004;16:116–21.
- [16] Wang JL, Birgisson B. A time domain boundary element method for modeling the quasi-static viscoelastic behavior of asphalt pavements. *Eng Anal Bound Elem* 2007;31:226–40.
- [17] Greengard LF, Rokhlin V. A fast algorithm for particle simulations. *J Comput Phys* 1987;73:325–48.
- [18] Greengard LF, Kropinski MC, Mayo A. Integral equation methods for Stokes flow and isotropic elasticity in the plane. *J Comput Phys* 1996;125:403–14.
- [19] Greengard LF, Helsing J. On the numerical evaluation of elastostatic fields in locally isotropic two-dimensional composites. *J Mech Phys Solids* 1998;46:1441–62.

- [20] Peirce AP, Napier JAL. A spectral multipole method for efficient solution of large-scale boundary element models in elastostatics. *Int J Numer Meth Eng* 1995;38:4009–34.
- [21] Yao Z, Kong F, Wang H, Wang P. 2D simulation of composite materials using BEM. *Eng Anal Bound Elem* 2004;28:927–35.
- [22] Wang H, Yao Z, Wang P. On the preconditioners for fast multipole boundary element methods for 2D multi-domain elastostatics. *Eng Anal Bound Elem* 2005;29:673–88.
- [23] Liu YJ, Nishimura N, Otani Y. Large-scale modeling of carbon-nanotube composites by the boundary element method based on a rigid-inclusion model. *Comput Mater Sci* 2005;34:173–87.
- [24] Liu YJ. A new fast multipole boundary element method for solving large-scale two-dimensional elastostatic problems. *Int J Numer Meth Eng* 2005;65:863–81.
- [25] Liu YJ, Nishimura N, Otani Y, Takahashi T, Chen XL, Munakata H. A fast boundary element method for the analysis of fiber-reinforced composites based on a rigid-inclusion model. *J Appl Mech* 2005;72:115–28.
- [26] Liu YJ. A fast multipole boundary element method for 2-D multi-domain elastostatic problems based on a dual BIE formulation. *Comput Mech* 2008;42:761–73.
- [27] Liu YJ. *Fast multipole boundary element method—theory and applications in engineering*. Cambridge: Cambridge University Press; 2009.
- [28] Lee SS, Westmann RA. Application of boundary element method to visco-elastic problems. In: Brebbia CA, Rencis JJ, editors. *Boundary element XV, vol. 2, Stress analysis*. Boston: Computational Mechanics Publications; 1993.
- [29] Lee SS. Boundary element analysis of linear viscoelastic problems using realistic relaxation functions. *Comput Struct* 1995;55(6):1027–36.
- [30] Melvin FK, Carl HP. *Advanced fracture mechanics*. New York: Oxford University Press; 1985.
- [31] Hu N, Wang B, Tan GW, Yao ZH, Yuan WF. Effective elastic properties of 2D solids with circular holes: numerical simulations. *Compos Sci Technol* 2000;60:1811–23.